Treatment of hind limb ischemia using angiogenic peptide nanofibers

Vivek A. Kumar[a], **Qi Liu**[b], **Navindee C. Wickremasinghe**[a], **Siyu Shi**[a], **Toya T. Cornwright**[b], **Yuxiao Deng**[b], **Alon Azares**[b], **Amanda N. Moore**[a], **Amanda M. Acevedo-Jake**[a], **Noel R. Agudo**[c], **Su Pan**[b], **Darren G. Woodside**[b], **Peter Vanderslice**[b], **James T. Willerson**[b], **Richard A. Dixon**[b,**], and **Jeffrey D. Hartgerink**[a,*]

[a] Department of Chemistry and Department of Bioengineering, Rice University, Houston, TX, USA

[b] Department of Molecular Cardiology, Texas Heart Institute, Houston, TX, USA

[c] Department of Pathology & Immunology, Baylor College of Medicine, Houston, TX, USA

Abstract

For a proangiogenic therapy to be successful, it must promote the development of mature vasculature for rapid reperfusion of ischemic tissue. Whole growth factor, stem cell, and gene therapies have yet to achieve the clinical success needed to become FDA-approved revascularization therapies. Herein, we characterize a biodegradable peptide-based scaffold engineered to mimic VEGF and self-assemble into a nanofibrous, thixotropic hydrogel, SLanc. We found that this injectable hydrogel was rapidly infiltrated by host cells and could be degraded while promoting the generation of neovessels. In mice with induced hind limb ischemia, this synthetic peptide scaffold promoted angiogenesis and ischemic tissue recovery, as shown by Doppler-quantified limb perfusion and a treadmill endurance test. Thirteen-month-old mice showed significant recovery within 7 days of treatment. Biodistribution studies in healthy mice showed that the hydrogel is safe when administered intramuscularly, subcutaneously, or intravenously. These preclinical studies help establish the efficacy of this treatment for peripheral artery disease due to diminished microvascular perfusion, a necessary step before clinical translation. This peptide-based approach eliminates the need for cell transplantation or viral gene transfection (therapies currently being assessed in clinical trials) and could be a more effective regenerative medicine approach to microvascular tissue engineering.

Keywords

Self-assembly; Therapeutic angiogenesis; Hind-limb ischemia; Multi-domain peptide; Peripheral artery disease

* Corresponding author. Department of Chemistry, Rice University, Mail Stop 602, 6100 Main St., Houston, TX 77030, USA. jdh@rice.edu (J.D. Hartgerink). ** Corresponding author. Department of Molecular Cardiology, Texas Heart Institute, PO Box 20345 C1000, Houston, TX 77030, USA. rdixon@texasheart.org (R.A. Dixon).

1. Introduction

Reduced blood flow to the symptomatic lower limbs of patients with peripheral artery disease (PAD) often results in limited mobility, pain, and potentially limb amputation. For many patients who have muscle pain during exercise (intermittent claudication), or critical limb ischemia, surgical intervention is contraindicated because of lack of collaterals, concomitant vascular disease, age, morbidity, or vascular access. For these patients and others in the early stages of PAD and that have ankle-brachial indices of 0.9–0.4, there is no FDA-approved revascularization therapy. Lower limb amputation is, therefore, often required [1–3].

Revascularization therapies should result in primary improvement in treadmill endurance and secondary improvement in perfusion. Strategies to promote blood vessel development have capitalized on stem cells and growth factors to recapitulate de novo niches for angiogenesis [1,2,4]. Current angiogenic strategies include delivering growth factors (eg, PDGF, PlGF, FGF, or VEGF) directly or via gene therapy, and administering stem cells [5–8]. However, low gene uptake, non-target transfection, immune rejection, and maladaptive inflammatory responses limit clinical translation [9–13]. For example, local delivery of VEGF or VEGF mimics results in modest reversal of ischemia or the development of leaky blood vessels, with much of the non-sequestered therapeutic draining through the lymphatics [7,8,13–15]. We describe, herein, the efficacy of an angiogenic mimic of VEGF anchored to a self-assembling multidomain peptide (MDP) for reversing disease progression in hind limb ischemia (HLI) through the development of stable, mature blood vessels. We call this peptide SLanc.

SLanc provides a unique platform for neovascularization. The fiber assembly process is accelerated by ionic charge screening with PO_{3-}^{4} buffer. The resulting thixotropic hydrogel is easily aspirated and delivered by syringe. In vivo, hydrogels are rapidly infiltrated by host cells and undergo neo-tissue remodeling with no fibrous encapsulation; allowing for excellent transport through implants [16–18]. We have previously shown that this peptide nanofiber hydrogel can modulate inflammation and promote angiogenesis [16–22]. SLanc has 3 key characteristics: controlled self-assembly into a nanofibrous hydrogel, an MMP-2 degradation sequence in the midblock of the peptide permitting enzymatic degradation, and a C-terminal mimic of VEGF [16,17,23] to promote angiogenesis. Thus, SLanc offers a powerful means to promote blood vessel growth in a degradable, extracellular matrix-mimetic polymer.

We previously injected SLanc subcutaneously into the dorsal aspect of healthy Wistar rats to determine the progression of hostdriven angiogenesis [17]. This model permitted evaluation of the host response with minimal influence from the reparative processes occurring in disease models. SLanc scaffolds undergo almost complete cellular infiltration within 3 days of treatment. Within 7 days, it was possible to detect mature microvasculature (25–75 μm in diameter) lined with smooth muscle cells. Cellular infiltration and angiogenesis within these subcutaneous implants led to implant degradation and replacement with native tissue within 3 weeks [17]. In the current study, we assessed SLanc's angiogenic potential, biodistribution, and therapeutic efficacy in treating ischemic tissue disease by using a PAD mouse model.

2. Materials and methods

2.1. Peptide synthesis and characterization

In a previous study [17], we designed a proangiogenic self-assembling VEGF mimic [SLanc: K-(SL)$_3$(RG)(SL)$_3$-K-G-KLTWQE-LYQLKYKGI] and a peptide without the angiogenic mimic [SLc: K$_2$-(SL)$_3$(RG)(SL)$_3$-K$_2$]. In the current study, we also synthesized SLanc with the TAMRA fluorophore conjugated to the N-terminus (F-SLanc). All peptides, resin, and coupling reagents were purchased from NovaBiochem (St. Louis, MO). Standard solid-phase peptide synthesis was performed with an Apex Focus XC synthesizer (AAPPTec, Louisville, KY), Rink amide resin with 0.37 mM loading, and N-terminal acetylation, except for F-SLanc. After each protein was cleaved from the resin, the crude mass was checked before dialysis was performed against deionized water using dialysis tubing with a molecular weight cut-off of 1000–2000 Da (Sigma-Aldrich, St. Louis, MO). The peptides were subsequently lyophilized, and their purity was confirmed by using electron-spray ionization mass spectrometry (MicroTOF ESI, Bruker Instruments, Billerica, MA). They were then reconstituted at 20 mg/mL in sterile 298 mM sucrose. Gelation of the peptides into thixotropic hydrogels was achieved by adding an equal volume of Hank's balanced salt solution (HBBS, pH 7.4).

Atomic force microscopy (AFM) and rheology testing were performed as previously reported [17–20]. Briefly, for AFM, the SLanc peptide solutions (0.01–0.05 wt%) were dropped onto spinning freshly cleaved mica. Images were collected in air at ambient temperature with a Digital Instruments Nanoscope IIIa in tapping mode. For the rheological analysis, 50 μL of 1 wt% thixotropic F-SLanc peptide hydrogel was plated on an 8-mm parallel plate geometry (gap 250 μm). Frequency sweep (0.1–100 Hz, at constant 1% strain), strain sweep (0–1000% strain, at 1 Hz), and shear recovery (1% strain for 30 min, 100% strain for 60 s, 1% strain for 30 min) were performed using an AR-G2 rheometer (TA Instruments, New Castle, DE). Phase angle was maintained at δ 90° to ensure no slipping. Four independent samples were analyzed.

Fluorescence stability was measured by aliquoting 200 μL of F-SLanc (1 wt%) into individual wells of a 96-well plate. Plates were incubated at 37 °C in a humidified incubator. Fluorescence was measured with an excitation wavelength of 540 nm and an emission wavelength of 570 nm on days 0, 1, 2, 4, 6, 9, 12, 15, 19, 23, 27, and 31. Four samples were analyzed.

2.2. VEGF competitive binding

Human umbilical vein endothelial cells (HUVECs) were plated in 24-well plates (50,000 cells per well) and grown until confluent. The cells were preconditioned in a low-serum (1%) medium for 5 h before the peptides were added. F-SLanc was dissolved in low-serum medium and added to the HUVECs at 1, 10, and 100 μM concentrations. The cells were placed on an incubator shaker at 40 rpm for 16 h. Then, the cells were treated with Liberase and analyzed by using fluorescence-activated cell sorting (FACS), as detailed below. Fluorescent peptide bound to the cells was blocked at 1 μM peptide loading by 100 ng/mL VEGF (Peprotech, Rocky Hill, NJ). Four independent samples were assessed.

2.3. In vivo biodistribution of F-SLanc

Animal procedures were conducted according to the Rice University Animal Welfare Committee guidelines and in accordance with the National Institutes of Health Guide for the Care and Use of Laboratory Animals. C57BL/6J mice (22–25 g) were purchased from Charles River Laboratories (Germantown, MA). The mice were anesthetized via isoflurane inhalation, and a depilatory cream was used to remove hair from the dorsal and ventral aspects to minimize autofluorescence. Then, the mice underwent subcutaneous (SC), intravenous (IV), or intramuscular (IM) injections of F-SLanc thixotropic gel (1 wt%). For the SC injections, 200 μL was injected into the dorsal aspect. For the IV injections, 200 μL was injected into the tail vein over a 10–20 s period. For the IM injections, 50 μL was injected into the quadriceps of the right leg. A 27-gauge needle was used for the SC and IM injections, and a 30-gauge needle was used for the IV injections. The mice were imaged at various timepoints using intravital fluorescent imaging (IVIS Lumina K Series III, PerkinElmer, Waltham, MA), and LiveImage 4.3.1 (PerkinElmer, Waltham, MA) was used for autofluorescence correction. All experiments were performed four times.

2.4. Evaluation of cellular infiltration

We retrieved the 200 μL SC SLanc hydrogel scaffolds by carefully removing the implants and trimming the surrounding fascia at day 7. The explants were washed in PBS and processed for either FACS or transmission electron microscopy (TEM) analysis. FACS samples were treated with Liberase (Roche Diagnostics, Indianapolis, IN) at 37 °C for 20 min total. Tissues were dissociated manually for 5 min by using pipet tips and a scalpel and were placed on a shaker in an incubator for 15 min at 37 °C. Cell suspensions were filtered through a 70-mm cell strainer, centrifuged, and resuspended in FACS buffer (PBS, 5 mM EDTA, and 1% bovine serum albumin). The cells were incubated with Fc receptor CD16/32 block (Becton Dickinson, Mountain View, CA) at 4 °C for 5 min, centrifuged, and resuspended in fresh FACS buffer. Then, they were stained with anti-CD45-VioBlue (Millipore, clone: 30F11) at the manufacturer's suggested dilution for 30 min at 4 °C. Flow cytometry was performed with a FACSCalibur (Becton Dickinson).

TEM samples were fixed with 2.5% glutaraldehyde in 0.1 M cacodylate buffer (pH 7.4) for 5 h at room temperature and then at 4 °C overnight. Afterwards, they were washed twice in 0.1 M cacodylate buffer. Samples were first stained with 1% osmium tetroxide in ddH2O for 30 min and washed in 0.1 M cacodylate buffer and ddH2O. Then, they were stained with 1% (wt/vol) uranyl acetate (aq) for 1 h and rinsed in ddH2O. Samples were subsequently dehydrated with an ethanol series, infiltrated with 100% resin, and allowed to polymerize for 3 d at 60 °C. A diamond knife was used to cut ultrathin (70 nm) sections. After being sectioned, the samples were stained with 3% uranyl acetate and Reynold's lead citrate and examined with TEM at an accelerating voltage of 80 keV.

2.5. Mouse unilateral hind limb ischemia model

Animal procedures were conducted according to the University of Texas Health Science Center Animal Welfare Committee guidelines and in accordance with the National Institutes of Health Guide for the Care and Use of Laboratory Animals. Eight-month-old and 13-month-old C57BL/6J mice were purchased from the Jackson Laboratory (Bar Harbor, ME).

Equal numbers of mice (sex- and age-matched) were randomly divided into 3 treatment cohorts: SLc peptide, SLanc peptide, or HBSS carrier control; n = 8 per group for the 8-month-old mice and n = 10 per group for the 13-month-old mice. The mice were anesthetized via inhalation of 2–4% isoflurane, and hind limb ischemia was induced with unilateral surgical ligation. For the procedure, 2 sutures were placed adjacent to each other on the left femoral artery, proximal to the origin of the femoral bifurcation, to interrupt blood flow. After ischemia was induced, the incision was closed, and the mice were returned to their cages. Twenty-four hours after the surgery, the mice were briefly anesthetized, and a total of 50 μL of peptide (SLc, SLanc or HBSS) was injected into the quadricep (25 μL) and gastrocnemius (25 μL) muscles of the ischemic hind limb.

2.6. Histology

Histological evaluation of muscle was performed as previously published [17]. Briefly, tissue was processed into paraffin blocks, cut into 7-mm sections, deparaffinized, and stained with hematoxylin and eosin or Masson's trichrome to characterize the tissue architecture and vasculature. Angiogenesis was detected with goat antimouse CD31 antibody (Santa Cruz Biotech, Santa Cruz, CA), smooth muscle cells were detected with rabbit anti-mouse a-SMA antibody (Genetex, Irvine, CA), and nucleic were visualized with DAPI counterstain. Secondary antibodies used were donkey anti-goat FITC (GeneTex) and donkey anti-rabbit AF 647 (Thermo Fisher Scientific, Waltham, MA).

2.7. Tissue recovery: Laser Doppler perfusion imaging and treadmill endurance test

As described previously [24], Laser Doppler imaging (Perimed AB, Järfallä, Sweden) was used to obtain serial measurements of perfusion. For the 8-month-old mice (n = 8 per group), measurements were taken on days 1, 3, 5, 7, 14, 21, 28, 60, and 90 after receiving IM injections of SLc, SLanc or vehicle (HBSS), and for the 13-month-old mice (n = 10 per group), measurements were obtained on days 1, 3, 5, 7, 14, 21, and 28 after the injections. Degree of reperfusion was expressed as the ratio of perfusion in the ischemic foot pad to that in the contralateral non-manipulated foot pad.

At various time points after treatment (days 28 and 90 for the 8-month-old mice and day 21 for the 13-month-old mice), all mice were challenged with acute exercise (run-to-exhaustion). Before the endurance test was begun, the mice were acclimated to the treadmill (Eco 3/6, Columbus Instruments, inclination +5°) for 1–2 h and to the motor sound for 15 min. For the test, the treadmill belt was started at a slow speed (6 m/min), and then the velocity was increased 2 m/min every 2 min for the initial 12 min and held constant at 18 m/min thereafter. Exhaustion was defined as when the mouse spent more than 10 consecutive seconds on the shock grid without trying to reengage the treadmill. The maximal running distances (in m) were recorded.

2.8. Statistical analysis

The data are shown as mean ± SD. The student's t-test was used to compare differences between paired data points, analysis of variance (ANOVA) with Tukey post hoc analysis was used for multiple comparisons of parametric data, and Kruskal-Wallis ANOVA with Dunn's

post hoc analysis was used for nonparametric data. *P* values < 0.05 were considered statistically significant.

3. Results

SLanc is synthesized at high purity (>90%, as determined by HPLC) (Fig. S1a), and undergoes self-assembly into a nanofibrous hydrogel through simultaneous hydrogen bond formation and hydrophobic packing (Fig. 1a). To evaluate biodistribution, we conjugated TAMRA to SLanc's N-terminus to produce a near IR peptide probe that could be fluorescently tracked in vivo (F-SLanc). Fig. 1b shows the sequences of all 3 synthesized peptides: SLanc, F-SLanc, and SLc (the base MDP without the VEGF mimic). Atomic force microscopy was used to demonstrate the nanofibrous structure of SLanc. F-SLanc exhibits thixotropic behavior (Fig. S2) and marked fluorophore stability at 37 °C in phosphate buffer, over 1 month (Fig. S3). VEGF mimic and SLanc binding to VEGF receptors has been previously demonstrated [17,25–28]. Here, F-SLanc binding to VEGF receptors on HUVECs was found to be dose-dependent; and inhibited by adding recombinant human VEGF (Fig. S4). These studies helped understand self-assembly and the pro-angiogenic activity that potentiates development of mature vessels [17].

To assess cellular infiltration into SLanc scaffolds in vivo, we administered the hydrogel (200 μL) subcutaneously into healthy C57BL/6J mice. At 7 days, we analyzed the isolated scaffolds by transmission electron microscopy (TEM) and flow cytometry. Gross morphology revealed large-diameter vessels within and a concentrated vascularized bed surrounding implants (Fig. 2a and b). TEM images of the Eponate-embedded implants showed collagen fibrils in close association with filamentous peptide (Fig. 2c). Signs of de novo extracellular matrix production and remodeling were seen in the center of the implants, indicating intimate contact between the native tissue and SLanc. The phagocytic infiltrate in the scaffolds had vacuoles containing peptide fragments, signifying intracellular degradation of the peptide scaffold (Fig. 2c–e). Peptides were seen in direct association with the cellular plasma membrane (Fig. 2f), which may have promoted VEGF receptor activation. To further characterize the cellular infiltrates, digested subcutaneous explants analyzed with flow cytometry showed rapid infiltration of CD45^{+} hematopoietic cells by day 7 (Fig. S5), complementing previous histologic findings showing infiltration of CD31^{+}, Nestin^{+}, and a-SMA^{+} cells [17].

Therapeutic utility was evaluated in a C57BL/6J HLI mouse model. Acute ischemia was achieved by left femoral artery ligation proximal to the femoral bifurcation (Fig. S6). After 24 h, compounds were injected into the quadricep (25 μL) and gastrocnemius (25 μL). Laser Doppler perfusion imaging (LDPI) was used to monitor recovery of blood flow in the mice, and running endurance measured functional recovery. LDPI of the footpad compared perfusion in the ischemic limb to the non-ischemic contralateral limb (Fig. 3a & Fig. S7). In SLanc-treated mice, perfusion of the ischemic leg was significantly restored within 21 days for 8-month-old mice and within 7 days for 13-month-old mice, compared to controls, and continued to improve throughout the study period (Fig. 3b and d). For 8-month-old SLanc-treated mice, the improvement in perfusion resulted in superior muscle preservation at 28 days and significantly greater treadmill endurance at 90 days (Fig. 3c). Similarly, for 13-

month-old SLanc-treated mice, treadmill endurance results at 21 days were similar to those of the animals tested before surgery and were significantly greater than those of the control animals (Fig. 3e). Histology of muscle from 13-month-old SLanc-treated mice on day 28 showed good preservation of tissue architecture and vasculature and staining indicative of mature blood vessels (CD31$^+$, a-SMA$^+$) in the vicinity of the injection site (Fig. 4a–c).

Safety of SLanc was evaluated with biodistribution and gross morphological analyses. Biodistribution was evaluated by administering F-SLanc subcutaneously (200 μL), intramuscularly (50 μL), or intravenously (200 μL). Large boluses implanted in the subcutaneous space persisted for up to 11 days (>95% of implant degraded by day 11, as measured with fluorescent counts) (Fig. 4d). Intramuscular injection in the quadriceps resulted in slower degradation and clearance of the peptide than subcutaneous bolus injections, possibly due to the greater density and diminished interstitial flow in the muscle, compared to the dorsum interstices (Fig. 4e). Thixotropy and hemodynamic shear did not lead to thromboembolic events after F-SLanc was injected intravenously (200 μL) at approximately 1/10th of the blood volume of mice. F-SLanc began filtering into the urinary bladder within 1 h and was excreted over the next 11 days (Fig. S8). Gross morphology of kidneys, brain, liver, heart, lungs, and injection site at day 14 showed no difference in organ size or occurrence of hematomas or thromboembolic events (data not shown).

4. Discussion

SLanc acts as a novel mimic of VEGF. Previous work has demonstrated the ability for SLanc to activate and upregulate angiogenic receptor expression (VEGFR1, VEGFR2, NP-1) in HUVEC [17]. In this study, we further showed the binding of SLanc to HUVEC in a competitive fashion to native VEGF. Through the process of self-assembly, we hypothesize the development of 3 important facets that potentiate the robust responses seen in vitro and in vivo [17]. First we note that injected hydrogels self-assemble in situ, providing a sustained and prolonged in vivo response. We note that hydrogels degrade over a 3 week period in vivo, and thus allow the development of mature vasculature. Interestingly, we have recently demonstrated that the propensity for hydrogels to promote a robust angiogenic response can also be modulated by the release of a variety of growth factors in a temporally controlled manner. In this related study, Wickremasinghe et al. showed the development of mature vasculature in similar hydrogel preparations by the temporally controlled release of PlGF-1 in liposomes [20,29]. Similar to this study, and previously published work, the ability for MDP to rapidly infiltrate cells creates a niche for the rapid (within 7 days) development of mature SMC lined microvessels. Second, the propensity for multidomain peptides to stimulate a biocompatible host-response that is characterized by rapid cellular infiltration, lack of fibrous encapsulation and deposition of host tissue ECM [17–19]. This further bolsters the ability for host-implant communication and potentiation of continued angiogenic signaling. Third, we demonstrate that functionally, the use of proangiogenic peptides, synthesized on the peptide backbone, delivered using this self-assembling vehicle, presents a novel mechanism for the treatment of HLI, with efficacy comparable and superior to previously reported [17].

Numerous models of HLI use younger mice (eg, 8–12 weeks old), which recover more effectively than older mice (eg, 8 or 13 months old) that have less proliferative cells and decreased auto-regenerative potential [30–33]. We evaluated ischemic recovery in older mice to better mimic the impaired healing processes in PAD patients (>55 years old) [30–34]. Endogenous healing responses were more pronounced in 8-month-old mice than in 13-month-old mice. However, reduced endogenous responses seen in 13-month-old mice helped establish the pro-angiogenic effects of SLanc. This was exemplified by the rapid recovery rate of 13-month-old mice, which showed a significant difference in perfusion within 7 days and a running endurance comparable to pre-surgery levels within 21 days. In studies using similar models but with younger mice (8–12 weeks old), injections of VEGF (or VEGF mimics), stem cells, or other growth factor/cytokine therapies into ischemic limbs typically resulted in 30–50% restoration of perfusion by day 28, as observed with our study controls [2,4,9,26,35–39]. In contrast, we saw close to 90% restoration of perfusion within 28 days in the older mice, which had decreased auto-regenerative and healing potential [25,40]. Importantly, reperfusion of the footpad suggests anastomosis of vessels from the proximal vasculature to those of the distal vasculature and the generation of collaterals, which allowed for reperfusion of both the ischemic ligation site and footpad.

5. Conclusion

We have previously shown that SLanc is capable of promoting a mature angiogenic response in the subcutaneous space of rats [17]. In the current study, this VEGF-mimicking peptide was evaluated in a PAD mouse model. After treatment, perfusion was rapidly restored and a significant improvement in running endurance was observed in adult and aged mice with induced acute limb ischemia, indicating preservation of tissue structure and function. These two improvements were significantly greater than those observed for comparable HLI models after treatment with therapies currently being tested in clinical trials [3,5,10,17,37,41,42]. Biodistribution studies demonstrated excellent biocompatibility of parenterally administered SLanc. This novel peptide may provide an exciting platform for ischemia treatment and regenerative medicine.

Supplementary Material

Refer to Web version on PubMed Central for supplementary material.

Acknowledgements

References

[1]. Hinchliffe RJ, Andros G, Apelqvist J, Bakker K, Friederichs S, Lammer J, et al. A systematic review of the effectiveness of revascularization of the ulcerated foot in patients with diabetes and peripheral arterial disease. Diabetes Metab. Res. Rev. 2012; 28(Suppl. 1):179–217. [PubMed: 22271740]

[2]. Cooke JP, Losordo DW. Modulating the vascular response to limb ischemia: angiogenic and cell therapies. Circ. Res. 2015; 116:1561–1578. [PubMed: 25908729]

[3]. Simons M, Alitalo K, Annex BH, Augustin HG, Beam C, Berk BC, et al. State-of-the-art methods for evaluation of angiogenesis and tissue vascularization: a scientific statement from the American Heart Association. Circ. Res. 2015; 116:e99–e132. [PubMed: 25931450]

[4]. Cooke JP, Chen Z. A compendium on peripheral arterial disease. Circ. Res. 2015; 116:1505–1508. [PubMed: 25908724]

[5]. Mohsin S, Wu JC, Sussman MA. Predicting the future with stem cells. Circulation. 2014; 129:136–138. [PubMed: 24249719]

[6]. Yasumura EG, Stilhano RS, Samoto VY, Matsumoto PK, de Carvalho LP, Valero Lapchik VB, et al. Treatment of mouse limb ischemia with an integrative hypoxia-responsive vector expressing the vascular endothelial growth factor gene. PLoS One. 2012; 7:e33944. [PubMed: 22470498]

[7]. Sun Q, Silva EA, Wang A, Fritton JC, Mooney DJ, Schaffler MB, et al. Sustained release of multiple growth factors from injectable polymeric system as a novel therapeutic approach towards angiogenesis. Pharm. Res. 2010; 27:264–271. [PubMed: 19953308]

[8]. Sun Q, Chen RR, Shen Y, Mooney DJ, Rajagopalan S, Grossman PM. Sustained vascular endothelial growth factor delivery enhances angiogenesis and perfusion in ischemic hind limb. Pharm. Res. 2005; 22:1110–1116. [PubMed: 16028011]

[9]. Giacca M, Zacchigna S. VEGF gene therapy: therapeutic angiogenesis in the clinic and beyond. Gene Ther. 2012; 19:622–629. [PubMed: 22378343]

[10]. Lu J, Pompili VJ, Das H. Neovascularization and hematopoietic stem cells. Cell Biochem. Biophys. 2013; 67:235–245. [PubMed: 22038301]

[11]. Katare R, Stroemer P, Hicks C, Stevanato L, Patel S, Corteling R, et al. Clinical-grade human neural stem cells promote reparative neovascularization in mouse models of hindlimb ischemia. Arterioscler. Thromb. Vasc. Biol. 2014; 34:408–418. [PubMed: 24202301]

[12]. Stewart DJ, Kutryk MJ, Fitchett D, Freeman M, Camack N, Su Y, et al. VEGF gene therapy fails to improve perfusion of ischemic myocardium in patients with advanced coronary disease: results of the NORTHERN trial. Mol. Ther. 2009; 17:1109–1115. [PubMed: 19352324]

[13]. Simon-Yarza T, Formiga FR, Tamayo E, Pelacho B, Prosper F, Blanco-Prieto MJ. Vascular endothelial growth factor-delivery systems for cardiac repair: an overview. Theranostics. 2012; 2:541–552. [PubMed: 22737191]

[14]. Webber MJ, Han X, Murthy SN, Rajangam K, Stupp SI, Lomasney JW. Capturing the stem cell paracrine effect using heparin-presenting nanofibres to treat cardiovascular diseases. J. Tissue Eng. Regen. Med. 2010; 4:600–610. [PubMed: 20222010]

[15]. Chen RR, Snow JK, Palmer JP, Lin AS, Duvall CL, Guldberg RE, et al. Host immune competence and local ischemia affects the functionality of engineered vasculature. Microcirculation. 2007; 14:77–88. [PubMed: 17365663]

[16]. Galler KM, Aulisa L, Regan KR, D'Souza RN, Hartgerink JD. Self-assembling multidomain peptide hydrogels: designed susceptibility to enzymatic cleavage allows enhanced cell migration and spreading. J. Am. Chem. Soc. 2010; 132:3217–3223. [PubMed: 20158218]

[17]. Kumar VA, Taylor NL, Shi S, Wang BK, Jalan AA, Kang MK, et al. Highly angiogenic peptide nanofibers. ACS Nano. 2015; 9:860–868. [PubMed: 25584521]

[18]. Kumar VA, Taylor NL, Shi S, Wickremasinghe NC, D'Souza RN, Hartgerink JD. Self-assembling multidomain peptides tailor biological responses through biphasic release. Biomaterials. 2015; 52:71–78. [PubMed: 25818414]

[19]. Kumar VA, Shi S, Wang BK, Li IC, Jalan AA, Sarkar B, et al. Drug-triggered and cross-linked self-assembling nanofibrous hydrogels. J. Am. Chem. Soc. 2015; 137:4823–4830. [PubMed: 25831137]

[20]. Wickremasinghe NC, Kumar VA, Hartgerink JD. Two-step self-assembly of liposome-multidomain peptide nanofiber hydrogel for time-controlled release. Biomacromolecules. 2014; 15:3587–3595. [PubMed: 25308335]

[21]. Wang Y, Bakota E, Chang BH, Entman M, Hartgerink JD, Danesh FR. Peptide nanofibers preconditioned with stem cell secretome are renoprotective. J. Am. Soc. Nephrol. 2011; 22:704–717. [PubMed: 21415151]

[22]. Bakota EL, Wang Y, Danesh FR, Hartgerink JD. Injectable multidomain peptide nanofiber hydrogel as a delivery agent for stem cell secretome. Biomacromolecules. 2011; 12:1651–1657. [PubMed: 21417437]

[23]. Bakota EL, Aulisa L, Galler KM, Hartgerink JD. Enzymatic cross-linking of a nanofibrous peptide hydrogel. Biomacromolecules. 2011; 12:82–87. [PubMed: 21133404]

[24]. Liu Q, Chen Z, Terry T, McNatt JM, Willerson JT, Zoldhelyi P. Intra-arterial transplantation of adult bone marrow cells restores blood flow and regenerates skeletal muscle in ischemic limbs. Vasc. Endovasc. Surg. 2009; 43:433–443.

[25]. Webber MJ, Tongers J, Newcomb CJ, Marquardt KT, Bauersachs J, Losordo DW, et al. Supramolecular nanostructures that mimic VEGF as a strategy for ischemic tissue repair. Proc. Natl. Acad. Sci. U. S. A. 2011; 108:13438–13443. [PubMed: 21808036]

[26]. Santulli G, Ciccarelli M, Palumbo G, Campanile A, Galasso G, Ziaco B, et al. In vivo properties of the proangiogenic peptide QK. J. Transl. Med. 2009; 7:41. [PubMed: 19505323]

[27]. D'Andrea LD, Iaccarino G, Fattorusso R, Sorriento D, Carannante C, Capasso D, et al. Targeting angiogenesis: structural characterization and biological properties of a de novo engineered VEGF mimicking peptide. Proc. Natl. Acad. Sci. U. S. A. 2005; 102:14215–14220. [PubMed: 16186493]

[28]. Finetti F, Basile A, Capasso D, Di Gaetano S, Di Stasi R, Pascale M, et al. Functional and pharmacological characterization of a VEGF mimetic peptide on reparative angiogenesis. Biochem. Pharmacol. 2012; 84:303–311. [PubMed: 22554565]

[29]. Wickremasinghe NC, Kumar VA, Shi S, Hartgerink JD. Controlled angiogenesis in peptide nanofiber composite hydrogels. ACS Biomater. Sci. Eng. 2015; 1:845–854. [PubMed: 26925462]

[30]. Fowkes FG, Rudan D, Rudan I, Aboyans V, Denenberg JO, McDermott MM, et al. Comparison of global estimates of prevalence and risk factors for peripheral artery disease in 2000 and 2010: a systematic review and analysis. Lancet. 2013; 382:1329–1340. [PubMed: 23915883]

[31]. Semenza GL. Oxygen sensing, homeostasis, and disease. N. Engl. J. Med. 2011; 365:537–547. [PubMed: 21830968]

[32]. Leosco D, Rengo G, Iaccarino G, Sanzari E, Golino L, De Lisa G, et al. Prior exercise improves age-dependent vascular endothelial growth factor down-regulation and angiogenesis responses to hind-limb ischemia in old rats. J. Gerontol. A Biol. Sci. Med. Sci. 2007; 62:471–480. [PubMed: 17522350]

[33]. Rivard A, Fabre JE, Silver M, Chen D, Murohara T, Kearney M, et al. Age-dependent impairment of angiogenesis. Circulation. 1999; 99:111–120. [PubMed: 9884387]

[34]. Wang H, Listrat A, Meunier B, Gueugneau M, Coudy-Gandilhon C, Combaret L, et al. Apoptosis in capillary endothelial cells in ageing skeletal muscle. Aging Cell. 2014; 13:254–262. [PubMed: 24245531]

[35]. Chan LY, Gunasekera S, Henriques ST, Worth NF, Le SJ, Clark RJ, et al. Engineering pro-angiogenic peptides using stable, disulfide-rich cyclic scaffolds. Blood. 2011; 118:6709–6717. [PubMed: 22039263]

[36]. Grochot-Przeczek A, Dulak J, Jozkowicz A. Therapeutic angiogenesis for revascularization in peripheral artery disease. Gene. 2013; 525:220–228. [PubMed: 23566831]

[37]. Phelps EA, Garcia AJ. Engineering more than a cell: vascularization strategies in tissue engineering. Curr. Opin. Biotechnol. 2010; 21:704–709. [PubMed: 20638268]

[38]. Phelps EA, Landazuri N, Thule PM, Taylor WR, Garcia AJ. Bioartificial matrices for therapeutic vascularization. Proc. Natl. Acad. Sci. U. S. A. 2010; 107:3323–3328. [PubMed: 20080569]

[39]. Terry T, Chen Z, Dixon RA, Vanderslice P, Zoldhelyi P, Willerson JT, et al. CD34(þ)/M-cadherin(þ) bone marrow progenitor cells promote arteriogenesis in ischemic hindlimbs of ApoE(−)/(−) mice. PLoS One. 2011; 6:e20673. [PubMed: 21677770]

[40]. Liu X, Terry T, Pan S, Yang Z, Willerson JT, Dixon RA, et al. Osmotic drug delivery to ischemic hindlimbs and perfusion of vasculature with microfil for micro-computed tomography imaging. J. Vis. Exp. 2013; 76:e50364. http://dx.doi.org/10.3791/50364.

[41]. Capoccia BJ, Robson DL, Levac KD, Maxwell DJ, Hohm SA, Neelamkavil MJ, et al. Revascularization of ischemic limbs after transplantation of human bone marrow cells with high aldehyde dehydrogenase activity. Blood. 2009; 113:5340–5351. [PubMed: 19324906]

[42]. Prather WR, Toren A, Meiron M, Ofir R, Tschope C, Horwitz EM. The role of placental-derived adherent stromal cell (PLX-PAD) in the treatment of critical limb ischemia. Cytotherapy. 2009; 11:427–434. [PubMed: 19526389]

Author Manuscript
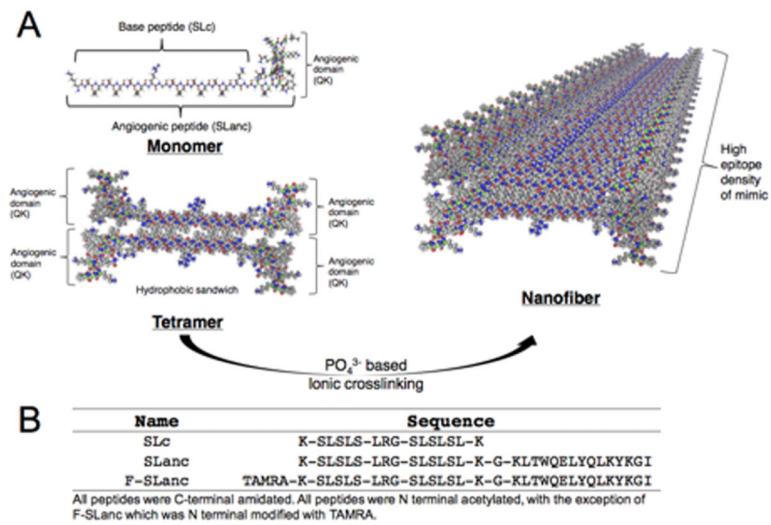
Author Manuscript

Author Manuscript

Author Manuscript

Fig. 1.
Self-assembly schematics and sequences of the peptides studied. (a) Schematics show how the polypeptides self-assemble through hydrophobic packing and hydrogen bonding along the fiber axis. (b) Sequences are shown for the peptides used in this study.
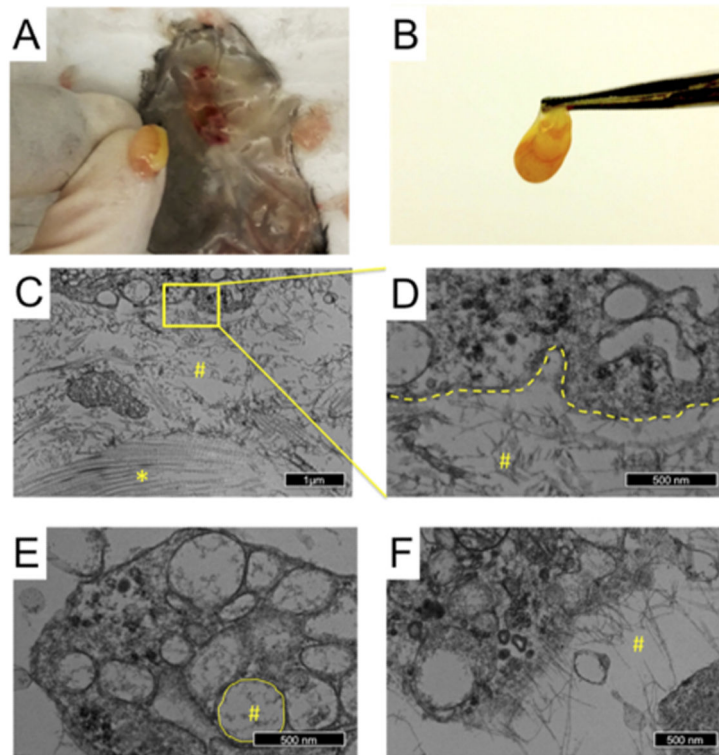
Fig. 2.
Characterization of the angiogenic peptide. The cellular response was determined by analyzing the subcutaneous thixotropic gel implants. (a, b) Vascular beds were found beneath (a) and around (b) the isolated implants. (cef) Transmission electron microscopy images of the cells that infiltrated the scaffolds in vivo showed invaginations of phagocytized peptide (c, d), present in intracellular vacuoles (e), and peptide organizing in the proximity of the plasma membrane (f). Peptide fibers are noted (#) in proximity with collagen (*) identified by their canonical D-periodicity in the center of the implants. Deposition of neo-matrix and indicates implant biocompatibility.
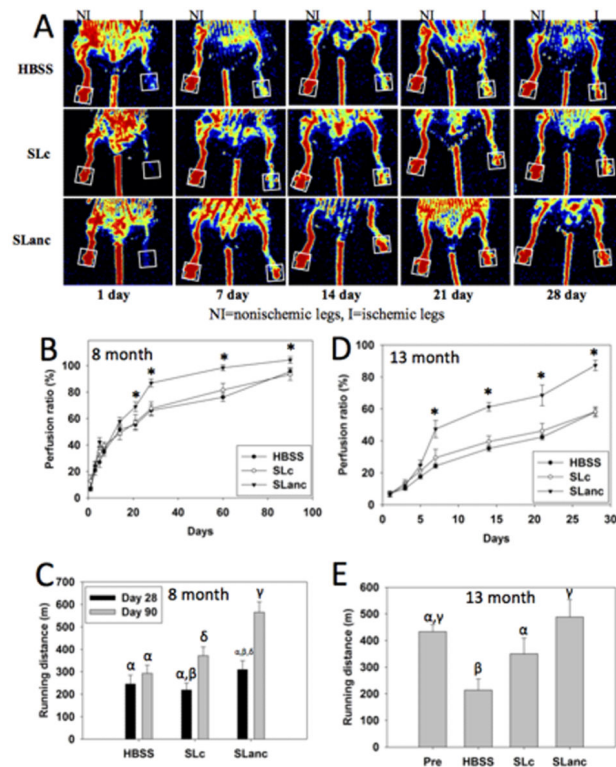
Fig. 3.

Recovery from hind limb ischemia after treatment with SLanc (angiogenic peptide), SLc (base peptide), or HBSS (carrier control). (a) Laser Doppler perfusion imaging (LDPI) showed rapid restoration of blood flow to the foot pad (boxed region) in SLanc-treated 13 month old mice, as compared to that in control SLc- and HBSS-treated mice. In 8-month-old mice, SLanc treatment resulted in significantly improved perfusion in the ischemic foot pad by day 21 after treatment (b) and significantly greater treadmill endurance by day 90 (c), as compared to that for SLc- and HBSS-treated mice. (d,e) Likewise, in 13-month-old mice, SLanc treatment resulted in significantly improved perfusion by day 7 after treatment (d) and significantly greater treadmill endurance by day 21 (e), as compared to that for SLc- and HBSS-treated mice. Columns labeled with different Greek letters and data points labeled with an asterisk (*) are statistically different from each other ($P < 0.05$). n = 8 per group for 8-month-old mice, and n = 10 per group for 13-month-old mice.
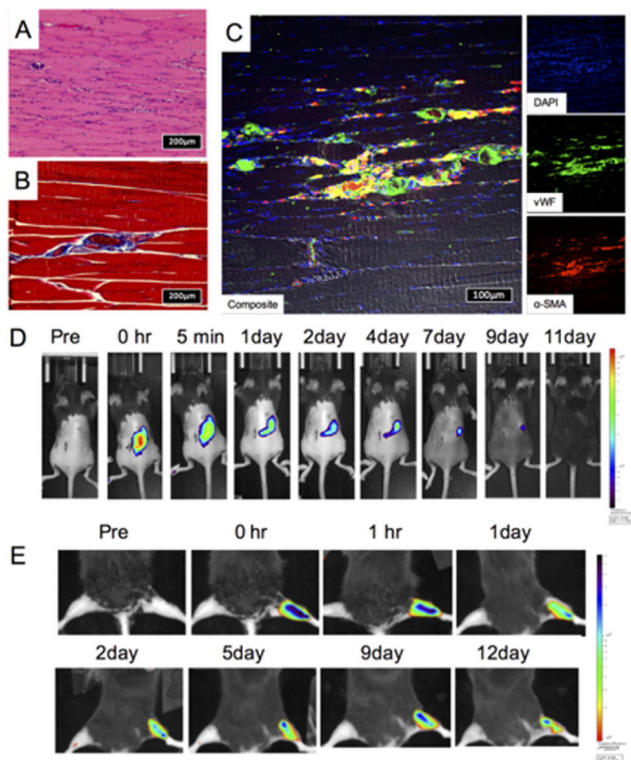
Fig. 4.
Histology of a reperfused muscle and biodistribution of SLanc. (a-c) Representative muscle tissue from a 13-month-old mouse with induced hind limb ischemia 28 days after treatment with SLanc showed muscle vitality in an H&E-stained section (a), development of mature blood vessels in the vicinity of the injection site in a Masson's Trichrome stained section (b), and the presence of endothelial cells (CD31) and smooth muscle cells (a-SMA) in an immunostained section (c). Nuclei are shown with DAPI staining. Biodistribution of SLanc in healthy C57BL/6 mice in a variety of routes: (d) subcutaneous SLanc implants (200 μL) degraded over a period of 11 days (>95% decrease seen in fluorescence intensity), while (e) intramuscular SLanc implants showed longer degradation rates, with biodegradable peptide persisting beyond 12 days, n = 4 for each delivery route.